

# An Innovative Method for Rotor Inertia Emulation at Wind Turbine Test Benches

U. Jassmann \* M. Reiter \* D. Abel \*

\* RWTH Aachen University, Institute of Automatic Control,  
52056 Aachen (Tel: +49 241-80 28033; e-mail:  
u.jassmann@irt.rwth-aachen.de).

**Abstract:** Recently wind industry paid a lot of attention to nacelle test benches in the multi MW class, which allow overall tests of wind turbine systems, including the control strategy. For several reasons the rotors of such turbines are dismantled at test benches, through which the dynamic properties of the system are changed significantly. This results in the challenge of having to emulate the missing rotational inertia for realistic wind turbine controller tests. In this paper an innovative method is proposed, which allows the emulation of the missing rotational inertia. The idea of the proposed method is to balance the inertia related torque by controlling the rotational impulse of the wind turbine's drive train. This has the advantage, that compared to a baseline approach, this method does not require a rigid drive train at the test bench to accurately emulate the rotor inertia. For this reason the proposed method reproduces the drive train's dynamics more accurately than the baseline approach and thereby allows for stable operation of the wind turbine controller. An experimental verification of the method was conducted at the world-wide first nacelle test bench.

Keywords: rotor inertia emulation, inertia simulation, rotational impulse control, hardware in the loop, wind energy, ground testing, nacelle test bench, drive train test bench

## 1. INTRODUCTION

The amount of world wide installed wind power increased in the last seven years by about 600 % according to the Global Wind Energy Council [February 2013] and is expected to keep growing throughout the next years. In the future wind energy will play a relevant role for the electrical power supply and the reliability of such will then also depend on the reliability of wind turbines. Therefore many manufacturer and also research institutes are investigating how test benches can help to assess and improve the reliability of wind turbines in an early stage of the development process. Recently more attention has been paid to overall system tests, where wind turbine nacelles or drive trains are put on test benches. Such ground testing facilities allow to investigate the interaction of all components, electrical and mechanical, within a wind turbine in specific load situations. In contrast to field tests this loads are reproducible and hence allow for very specific tests necessary to asses reliability.

Generally this ground testing facilities can be divided into two categories: drive train and nacelle test benches. While drive train test benches do not take into account the influence of the wind turbine's controller, nacelle test benches do. In both cases the wind turbine is mounted to the test bench without the rotor, which represents the major portion of the rotational inertia of the drive train and therefore specifies its dynamical behaviour significantly. For this reason the emulation of the rotational inertia is crucial for realistic test results. For nacelle test benches the accurate emulation is even more important, since the drive train represents the plant in the speed control loop

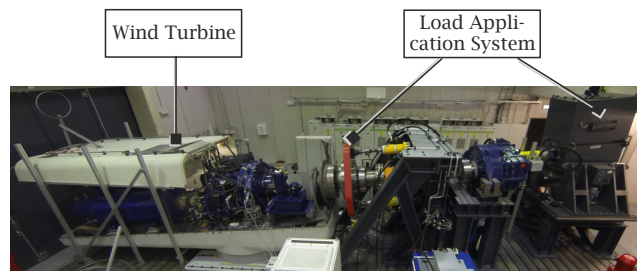


Fig. 1. Photograph of the 1MW nacelle test bench used to obtain experimental results.

of the wind turbine's controller, which has to run in stable operation without any parameter being changed.

In this paper the emulation of missing rotational inertia for the operation of wind turbines at nacelle test benches is addressed. A baseline approach and its downside for the given problem will be used to motivate the necessity for the new emulation method proposed in this paper. Both methods are tested at a 1 MW nacelle test bench available at the CENTER FOR WIND POWER DRIVES (CWD) of RWTH Aachen University and shown in figure 1.

This paper is organized as follows: Within section 2 the ground testing facility referred to in this paper will be described before in section 3 the necessity for inertia emulation is further motivated. In section 4 a test bench model is introduced, which is the basis for the investigations in section 5. In that section a baseline approach, called the *intuitive method* throughout this paper, and the proposed *new method* for the emulation of missing rotational inertia

are presented and compared to each other. Conclusions will be drawn in section 6.

## 2. NACELLE TEST BENCH

The 1MW nacelle test bench used for experiments throughout this paper was launched at the beginning of 2013 and is composed as shown in figure 2. Three physical systems need to be reproduced to operate the wind turbine in the artificial environment of the nacelle test bench. Those are the

- Mechanical
- Electrical and
- Auxiliary system.

These systems are linked to each other on signal level through the Global Test Bench Controller on one hand, and on physical level via the wind turbine under test on the other hand.

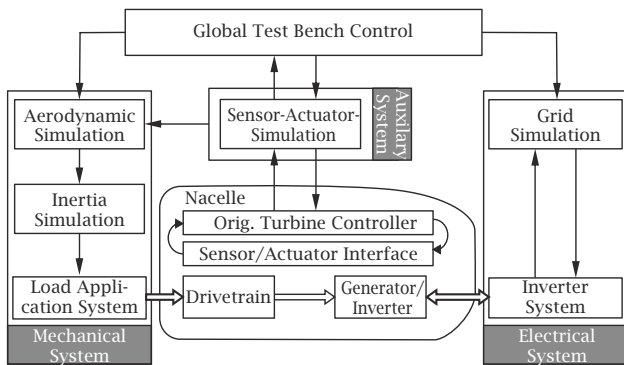


Fig. 2. Sketch of the composition and interactions of the three implemented HiL-simulations and the wind turbine.

The mechanical system contains a simulation of the aerodynamic properties of the rotor. This calculates torques and forces induced at the hub of the rotor, depending on the user defined wind speed, turbulence and direction as well as the measured rotational speed and pitch angle. Furthermore the simulation of the missing rotor inertia, which basically counteracts the aerodynamic torque, is part of the mechanical system. The resulting torques and forces are applied by a load application system. This consists of a driving motor with a rated power of 1 MW, which applies the rotational torque, and an extra non-torque load application system further described by Bosse et al. [2013]. Electrically the wind turbine is connected to an inverter based 50 Hz grid. These inverters are controlled by a real-time grid simulation, able to reproduce different grid failure states at the point of common coupling of the wind turbine. This assembly is depicted as electrical system in figure 2. Further details about the electrical system and its fault-ride-through capability are given by Helmedag et al. [2013].

Missing auxiliary components, which include any missing actuators or sensors, e.g. yaw motors or wind vane, are reproduced by a sensor-actuator simulation to provide corresponding feedback signals to the wind turbine's con-

troller and simulate state depended actuator behaviour such as for the pitch system.

For the emulation of the missing rotational inertia is the main focus of this paper, only the inertia simulation and the dynamic behavior of the driving motor in combination with the drive train are discussed and described further. The aerodynamic torque is considered as arbitrary input. The electrical and the auxiliary system are also beyond the scope of this paper.

## 3. MOTIVATION

The drive train of a wind turbine consists of the rotor, the shaft, the gearbox and the generator. Thereby the rotor contributes the most to the rotational inertia of the drive train. For this reason the inertia of the drive train is generally divided into the rotor inertia  $I_R$  and the inertia of the leftover drive train  $I_{DT}$  as among many others Wright [2004] and Henriksen [2010] propose. The driving torque of this system is the aerodynamic torque  $T_A$ , resulting from the wind speed, which is counteracted by the generator torque  $T_G$ , so that the rotational speed  $\omega$  results, as shown in figure 3.

When the wind turbine is mounted at the nacelle test bench the described wind turbine partitioning can also be interpreted as the *virtual system* and the *real system*, as shown in figure 3. The *real system* thereby represents the leftover drive train  $I_{DT}$  of the wind turbine, which is still physically present at the test bench. The aerodynamic torque  $T_A$  and the rotor  $I_R$  are denoted as *virtual system*, for they are not available but emulated. This *virtual system* has to provide the internal torque  $T^*$ , which is applied to the leftover drive train. It differs from the aerodynamic torque  $T_A$  by the impact the inertia  $I_R$  of the rotor has.

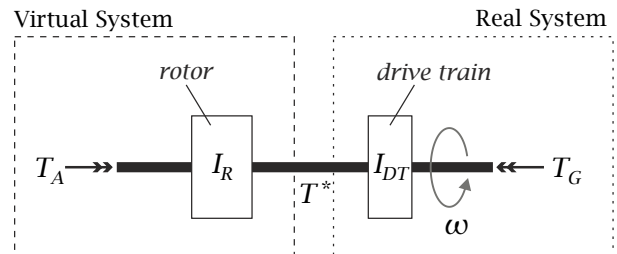


Fig. 3. Simplified diagram of the drive train of a wind turbine.

Intuitively the following equation can be considered to describe the given system:

$$T_A - T_G = (I_R + I_{DT}) \cdot \dot{\omega} \quad (1)$$

According to this the rotation speed  $\omega$  can be obtained by simply integrating (1), when the generator torque  $T_G$  is known. But as a generic test bench it should be operated without measuring the generator torque within the turbine. In this way the effort for testing different turbines is little. Moreover the wind turbine controls the rotation speed  $\omega$ , which is why the driving motor of the test bench is operated in torque mode and the internal torque  $T^*$  is to be obtained by the emulation and not the rotation speed  $\omega$ .

The only measurement available for the emulation is the

rotation speed  $\omega$ , as it can easily be measured. Given this, the internal torque  $T^*$  can be derived from (1) as

$$T^* = T_A - I_R \cdot \dot{\omega} \quad (2)$$

In combination with a filter, this solution can emulate the missing rotational inertia with sufficient quality for a drive train test bench, aiming at mechanical testing only. As, at nacelle test benches, the controller of the wind turbine is activated, the rotation speed  $\omega$  is controlled by adjusting the aerodynamic torque  $T_A$ . It will be shown in section 5.1, that this speed control loop is unstable if the *intuitive method* of (2) is used. Therefore it does not allow to operate a wind turbine at a nacelle test bench.

For this reason a *new method*, which allows the emulation of the missing rotational inertia sufficiently enough to operate drive train test benches as well as nacelle test benches, is required and will be proposed in section 5.2.

In order to compare both methods on a theoretical basis, a model of the dynamic behavior of the test bench is derived in the next section.

#### 4. TEST BENCH MODEL

The complete drive train present at the test bench is a combination of the wind turbine's leftover drive train  $I_{DT}$  and the test bench related drive train  $I_{TB}$ , which consists of the driving motor and the gearbox. Those two drive trains are connected via a low speed shaft. Both, the wind turbine related drive train and the test bench related drive train contain a gearbox, which is why their connection can not be considered as stiff. Therefore it is

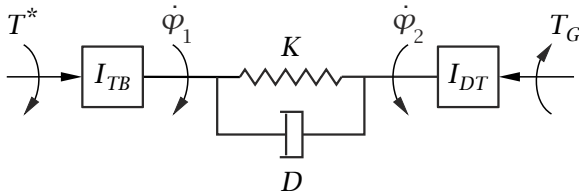


Fig. 4. Schematic of the flexible test bench model.

assumed that the drive trains of the test bench  $I_{TB}$  and the wind turbine  $I_{DT}$  are connected by a spring and damper system, which results in two different rotation speeds  $\dot{\varphi}_1$  and  $\dot{\varphi}_2$ , as depicted in figure 4. The internal torque  $T^*$  is considered as input to the test bench, while the generator torque  $T_G$  is counteracting. This system can be described by the following equations:

$$\begin{bmatrix} \dot{\varphi}_1 \\ \dot{\varphi}_2 \\ \Delta\dot{\varphi} \end{bmatrix} = \begin{bmatrix} -D/I_{TB} & D/I_{TB} & -K/I_{TB} \\ D/I_{DT} & -D/I_{DT} & K/I_{DT} \\ 1 & -1 & 0 \end{bmatrix} \begin{bmatrix} \varphi_1 \\ \varphi_2 \\ \Delta\varphi \end{bmatrix} + \begin{bmatrix} 1/I_{TB} & 0 \\ 0 & 1/I_{DT} \\ 0 & 0 \end{bmatrix} \begin{bmatrix} T^* \\ T_G \end{bmatrix} \quad (3)$$

The parameters for damping ( $D$ ), stiffness ( $K$ ) and inertias ( $I_{TB}$  and  $I_{DT}$ ) were identified via simulations and verified with measurements. From (3) the transfer function

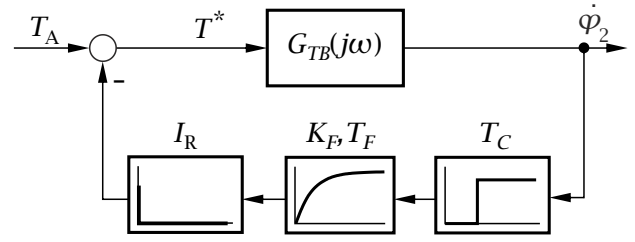


Fig. 5. Emulation loop of the intuitive method.

$$G_{TB}(j\omega) = \frac{\dot{\varphi}_2(j\omega)}{T^*(j\omega)} \quad (4)$$

$$= \frac{(D \cdot (j\omega) + K)/I_p}{(j\omega)^3 + D \cdot I_s(j\omega)^2 + K \cdot I_s(j\omega)} \quad (5)$$

with

$$I_p = I_{TB} \cdot I_{DT}$$

$$I_s = \frac{I_{TB} + I_{DT}}{I_{TB} \cdot I_{DT}}$$

can be derived, when  $T_G$  is set to zero. This transfer function will be used to analyse and compare the *intuitive* and the *new method* on a theoretical basis.

#### 5. EMULATION OF ROTATIONAL INERTIA

Within this section two procedures for the emulation of the missing rotational inertia  $I_R$  will be discussed. The first procedure has partly been introduced in section 3 and is called the *intuitive method*. The second procedure is firstly proposed in this paper and will be called the *new method*.

##### 5.1 Intuitive Method

In section 3 it was shown that the internal torque  $T^*$  of the real wind turbine can be obtained using (2). The required rotation speed  $\omega$  equals  $\dot{\varphi}_2$  of the test bench model (3),(4). Thus (2) becomes

$$T^* = T_A - I_R \cdot \dot{\varphi}_2 \quad (6)$$

Due to measurement noise the differentiator of (6) needs to be accompanied by a filter. Here a simple first order

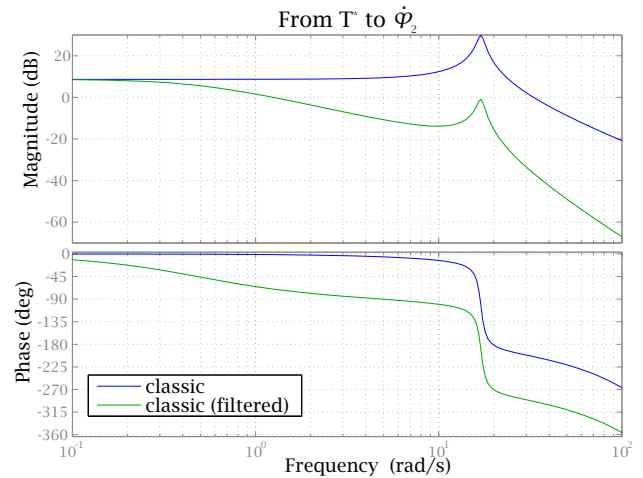


Fig. 6. bode plot of the intuitive method's open loops, for filter time constants  $T_F = 0$  and  $T_F \neq 0$ .

filter is used, so that the emulation loop shown in figure 5 results. For a filter with the gain  $K_F = 1$  and the time constant  $T_F$ , the open loop of the *intuitive method* can be denoted as

$$G_{0-1}(j\omega) = G_{TB}(j\omega) \cdot \frac{I_R \cdot (j\omega)}{(T_F \cdot (j\omega) + 1)} \cdot e^{(-j\omega \cdot T_c)}. \quad (7)$$

The time delay  $T_c$  is caused by the communication path and more than one order below the significant system dynamics. It is introduced here for the sake of completeness but will be neglected throughout the next equations, to avoid unnecessary confusion. Nonetheless the time delay is included in all bode plots.

In figure 6 the bode plots of the open loop  $G_{0-1}(j\omega)$  for a filter with a time constant  $T_F \neq 0$  (green) and  $T_F = 0$  (blue) are compared. The graph of the unfiltered open loop indicates, that the closed loop

$$G_{p-1}(j\omega) = \frac{\varphi_2(j\omega)}{T_A(j\omega)} \quad (8)$$

$$= \frac{G_{TB}(j\omega)}{1 + G_{0-1}(j\omega)} \\ = \frac{G_{TB}(j\omega) \cdot (T_F \cdot (\omega) + 1)}{(T_F + G_{TB}(j\omega) \cdot I_R) \cdot (j\omega) + 1} \quad (9)$$

of this system will be unstable according to the Nyquist criteria. If the time constant  $T_F$  of the filter is chosen high enough the closed loop  $G_{p-1}(j\omega)$  is stable as indicated by the green graph.

In general, the stability of  $G_{p-1}(j\omega)$  depends significantly on the ratio  $I_R/I_{DT}$ , which is proportional to the gain of  $G_{0-1}(j\omega)$  in (7). If this ratio is small enough  $G_{p-1}(j\omega)$  will be stable. But for an increasing ratio  $I_R/I_{DT}$  the system approaches the stability border. For the given system, where the missing inertia  $I_R$  is significantly higher than the leftover inertia  $I_{DT}$  the system becomes unstable.

The presented stable emulation loop  $G_{p-1}(j\omega)$  already allows to operate drive train test benches. For a given input torque  $T_A$ , the rotation speed  $\dot{\varphi}_2$  will appear accordingly to the given rotational inertia  $I_R$ . As, at nacelle test benches, the wind turbine's controller is activated, a speed controller  $G_{TC}(j\omega)$  closes a control loop from  $\dot{\varphi}_2$  to  $T_A$  as shown in figure 7.

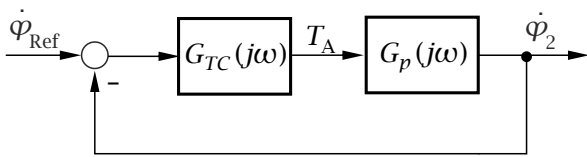


Fig. 7. Control loop closed by the wind turbine's controller  $G_{TC}(j\omega)$ .

Due to confidentiality the original parameters of such controller are unknown in general, hence an exact theoretical stability analysis is not possible. Instead experimental results shall be used at first to assess stability of the closed loop shown in figure 7. To do so, the presented *intuitive method* is implemented within the inertia simulation block at the test bench (see figure 2).

The experimental results are shown in figure 8. The top plot shows the pitch angle, which can be considered as proportional to the aerodynamic torque  $T_A$ . The bottom plot

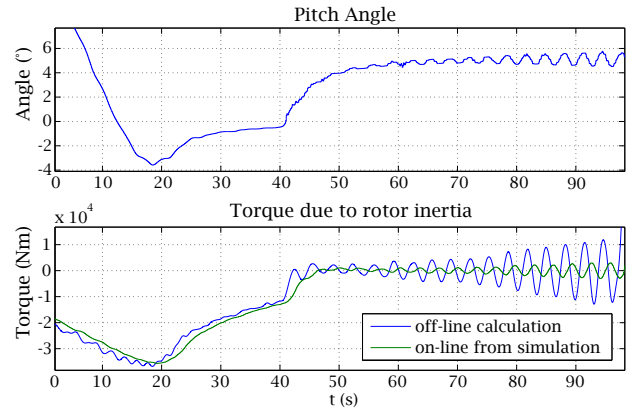


Fig. 8. Experimental results using the *intuitive method* for rotor inertia emulation.

shows a comparison of the on-line and off-line calculated share the rotational inertia  $I_R$  has in the internal torque  $T^*$  (See equation (6)). Looking at the control variable pitch angle, it is obvious that the speed control loop of the wind turbine (figure 7) becomes unstable, when the *intuitive method* is applied. In the bottom plot the green curve represents the on-line calculated inertia related torque  $\varphi_2 \cdot I_R$ , of the intuitive simulation loop pictured in figure 5. The off-line solution in blue was calculated using a phase lag free filtered rotation speed  $\dot{\varphi}_2$ . Considering the off-line solution as physical correct the on-line result of the *intuitive method* suffers a significant phase shift, caused by the filter. This is why the rotor's reaction is too retarded, and the controller cannot set the rotation speed as desired.

## 5.2 New Method

The assumption wrongfully made by the *intuitive method* in (1) is, that the drive train at the test bench is rigid. Thereby it is implied, that the measured rotation speed  $\dot{\varphi}_2$  used to solve (6) matches the system behaviour at any time. Hence the calculated internal torque  $T^*$  is also supposed to be correct at any time.

Other than this, the idea of the *new method* is, that the desired internal torque  $T^*$  and the aerodynamic torque  $T_A$  are leveled out over time, but not instantaneously. For that purpose the difference of these torques is integrated to a virtual rotation speed  $\dot{\varphi}_R$ . Its difference to the measured

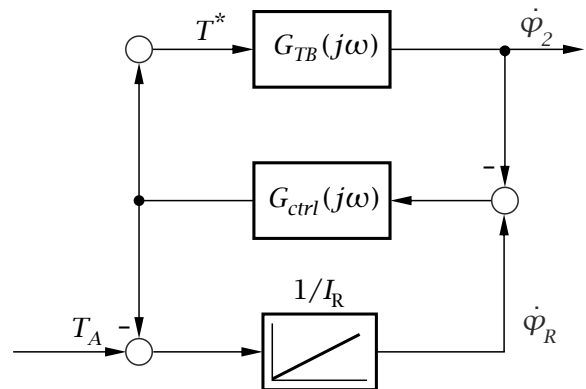


Fig. 9. Principal scheme of the *new method* for inertia emulation.

rotation speed  $\dot{\varphi}_2$  is forwarded to an arbitrary controller as shown in figure 9, which then provides the desired internal torque  $T^*$  as reference to the driving motor of the test bench. The difference between the internal torque  $T^*$  and the aerodynamic torque  $T_A$  can be interpreted as the share of the rotational inertia  $I_R$  in the internal torque  $T^*$ .

A more practical interpretation of the *new method* is, that the rotational impulse (energy) of the system is controlled and leveled out over time. Therefore the internal torque  $T^*$  is not absolutely correct at each simulation time step. In contrast the *intuitive method* tries to control the flow of the rotational impulse (power), in order to keep the internal torque  $T^*$  correct at each time step, which is unnecessary, since the simulation step size is about two orders smaller than the time constants of the emulated mechanical system.

Let the controller of the *new method* be a simple proportional gain, such that

$$G_{ctrl}(j\omega) = K_R \quad (10)$$

holds. In this case, the rotation speeds  $\dot{\varphi}_R$  and  $\dot{\varphi}_2$  are not to be equalized, so that no conflict with the speed controller of the wind turbine is evoked.

The open loop of this simulation loop has the form:

$$G_{0-2}(j\omega) = G_{TB}(j\omega) \cdot \frac{I_R \cdot (j\omega)}{\frac{I_R}{K_R} \cdot (j\omega) + 1} \quad (11)$$

When the proportional gain is chosen as  $K_R = I_R/T_F$  the open loop of the *new method* is equal to the open loop of the *intuitive method* in (7). Therefore it has the same stability issues as the intuitive solution and does work properly for drive train test benches

The difference between both methods is only revealed when the plant  $G_{p-i}(j\omega)$ , which is part of the open loop of the wind turbine's control loop (see figure 7), is considered. Using the *new method*  $G_{p-2}(j\omega)$  has the form:

$$G_{p-2}(j\omega) = \frac{G_{TB}(j\omega)}{1 + \frac{1}{I_R \cdot K_R} \cdot (1 + K_R \cdot G_{TB}(j\omega))(j\omega)} \quad (12)$$

Before examining the experimental results of the *new method*, as done for the *intuitive method*, both methods are compared qualitatively in the frequency domain. Therefore the open loop  $G_{0-3}(j\omega)$  of the wind turbine's speed control loop, shown in figure 7, can be considered as:

$$G_{0-WT}(j\omega) = G_{TC}(j\omega) \cdot G_{p-i}(j\omega) \quad (13)$$

For the *intuitive method*  $G_{p-i}(j\omega)$  is replaced by  $G_{p-1}(j\omega)$  (9), while for the *new method* it is replaced by  $G_{p-2}(j\omega)$  (12). The analysis is drawn with proportional control action  $G_{TC}(j\omega)$ , although the state of the art wind turbine controller is a PID-type control as Shan et al. [2013], Munteanu et al. [2008] and Hansen et al. [2005] suggest. Anyhow for both types of controller the qualitative same bode plot results and thus, for the sake of simplicity, the proportional controller is used. Furthermore the frequency response of the drive train of the real wind turbine is used as reference for the comparison of the methods. The bode plots of all three open loops are shown in figure 10.

It is evident, that in terms of stationary behaviour the presented methods are both equal to the real wind turbine. A difference can be noticed starting at about 1 rad/s,

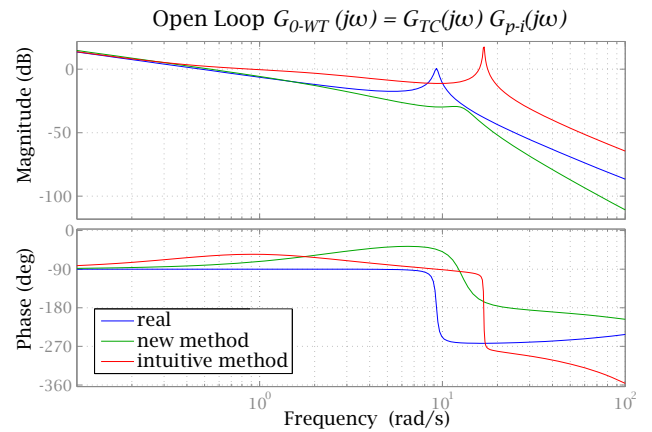


Fig. 10. Comparison of the frequency response of the real wind turbine and the two methods.

where the magnitude of the amplitude, using the *intuitive method*, is continuously above the magnitude of the real wind turbine, leading to additional sensitivity. Furthermore the *intuitive method* shifted the natural frequency to higher values and noticeably decreases damping. Although the wind turbine controller chosen is exemplary, it can be assumed, that this causes the instability seen in the experimental results in figure 8.

Compared to this, the magnitude of the *new method* is permanently below the magnitude of the real wind turbine and stability issues are not to be expected. Furthermore no resonance amplification is apparent at higher frequencies. Unfortunately the natural frequency present at the real wind turbine is also not reproduced by the *new method*, which lets the drive train appear more rigid than it really is.

Despite this drawback, the *new method* allows a wind turbine to be operated at the nacelle test bench. It reproduces the plant behavior, as expected by the speed controller  $G_{TC}(j\omega)$  of the wind turbine sufficiently enough to operate the control loop in figure 7 stably. This can be seen in figure 11, where a snippet of the start-up procedure of the turbine is plotted. Since the two inertia simulations have different dynamic behavior and no changes can be made to the wind turbine's start-up procedure and to the control parameters, the control actions in figure 11 are not

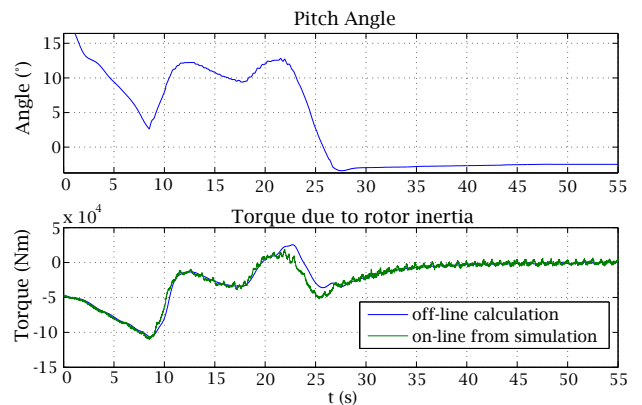


Fig. 11. Experimental results using the *new method* for rotor inertia emulation.

perfectly equal to the one of figure 8, as would be desired for easy comparison. Therefore characteristic points will be compared qualitatively.

Other than the start-up procedure with activated *intuitive method* in (figure 8), no significant phase lag of the inertia related torque is caused by the *new method*. For comparison the change of direction of the pitch angle can be considered, which happens at  $t = 8$  s in figure 11 and corresponds to  $t = 20$  s in figure 8.

Another interesting effect of the *new method* can be observed around  $t = 23$  s. At this moment the off-line calculated share of the rotational inertia  $I_R$  differs from the on-line solution of the *new method*. The on-line solution changes accordingly to the pitch angle of the top plot, which is proportional to the aerodynamic torque  $T_A$ . The difference of the off-line solution is caused by the generator torque  $T_G$ . At this moment the generator of the wind turbine is connected to the grid and accelerates the drive train. Thus external rotational energy is pumped into the system, which is not noticed by the proposed emulation method. After only a few seconds this difference is regulated and the rotational impulse in the system is balanced again.

Furthermore, the *new method* allows for higher, but realistic dynamics in the internal torque  $T^*$ , so that the influence of the tower shadow in the aerodynamic torque  $T_A$  can be reproduced nicely at the nacelle test bench as figure 11 shows.

## 6. SUMMARY AND CONCLUSION

In this paper a *new method* for the emulation of missing rotational inertia was presented, which allows the stable operation of wind turbines at nacelle test benches. It was shown that this method reproduced the dynamic behaviour of the wind turbine not perfectly for all frequencies, but more accurately than the *intuitive method*. Beside a theoretical justification of stability of the emulation loop of the *new method*, experimental results, derived from the operation of an 1 MW test bench, emphasized the advantage of the *new method*. Especially when it comes to external disturbances for instance by the generator, which are not noticeable by the emulation method, the *new method* reveals robustness.

Another advantage is, that actuator saturations as for the torque  $T^*$  can be incorporated into the emulation loop of the *new method*, such that only the really outputted value is used for the simulation and e.g. no wind-up effects appear.

Furthermore the *new method* allows to reproduce aerodynamic effects of higher dynamic, such as tower shadow.

In future work the mechanical dynamics of the blades have to replace the current lumped mass approach, in order to derive more realistic results. It is also planned to enhance the method, such that the first eigenfrequency of the wind turbine's drive train can be reproduced accurately at the nacelle test bench. Only then state of the art wind turbine controller, which actively damp this eigenfrequency, can be fully tested at the nacelle test bench. It is also undeniable that the first eigenfrequency plays a relevant role for the loads occurring in the components of the wind turbine.

## ACKNOWLEDGEMENTS

The depicted research is part of the project 'Verbesserung des Betriebsverhaltens von On-Shore Windenergieanlagen mithilfe eines neuartigen Systemprüfstandes' and partly supported by the European Union within the framework of the *European Regional Development Fund*.



EUROPEAN UNION  
Investing in Your Future  
European Regional  
Development Fund 2007-13

## REFERENCES

- Dennis Bosse, Friderike Barenhorst, Dominik Radner, and Ralf Schelenz. Analysis and application of iec61400 orientated wind loads for full scale ground testing. In *Conference for Wind Power Drives*, 2013.
- Global Wind Energy Council. Global wind statistics 2012, February 2013. Brüssel.
- M.H. Hansen, A. Hansen, T.J. Larsen, S. ye, and P. Srensen and P. Fuglsang. Control design for a pitch-regulated, variable speed wind turbine. Technical report, Technical Report Riso-R 1500, 2005.
- Alexander Helmedag, Timo Isermann, and Antonello Monti. Fault ride through certification of wind turbines based on a power hardware in the loop setup. In *Applied Measurements for Power Systems (AMPS), 2013 IEEE International Workshop on*, pages 150–155, 2013. doi: 10.1109/AMPS.2013.6656242.
- Lars Henriksen. *Model Predictive Control of Wind Turbines*. PhD thesis, Technical University of Denmark Informatics and Mathematical Modelling Building 321, DK-2800 Kongens Lyngby, Denmark, 2010.
- Iulian Munteanu, Nicolas-Antonio Cutululis, Antoneta Iuliana Bratcu, and Emil Ceanga. *Optimal Control of Wind Energy Systems*. Springer, 2008.
- Martin Shan, Boris Fischer, and Philipp Brosche. Regelungsentwurf für windenergieanlagen. at - *Automatisierungstechnik Methoden und Anwendungen der Steuerungs- Regelungs- und Informationstechnik*, 61: 305–317, 2013.
- A.D. Wright. Modern control design for flexible wind turbines. Technical report, Technical Report, NREL/TP-500-35816, 2004.